MURDOCH RESEARCH REPOSITORY

Nicol, M.J., Tjandrawan, V. and Zhang, S. (2016) Cathodic reduction of iron(III) and copper(II) on various sulfide minerals in chloride solutions. Hydrometallurgy, 166 . pp. 113-122.

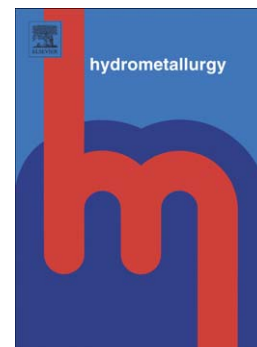http://researchrepository.murdoch.edu.au/id/eprint/34345/

Accepted Manuscript

Cathodic reduction of iron(III) and copper(II) on various sulfide minerals in chloride solutions

Michael J Nicol, Venny Tjandrawan, Suchun Zhang

Cathodic Reduction of Iron(III) and Copper(II) on Various Sulfide Minerals in Chloride Solutions

Michael J Nicol[1], Venny Tjandrawan[1] and Suchun Zhang[1]

1. *School of Engineering and Information Technology, Murdoch University, Perth, WA 6150, Australia*

Abstract

A comparative study of the electrochemical reduction of iron(III) and copper(II) ions on selected sulfide minerals in concentrated chloride solutions has been carried out as part of a broader study of the kinetics of the leaching of chalcopyrite, covellite, enargite and pyrite under chloride heap leaching conditions. Mixed potential, cyclic voltammetric and potentiostatic measurements have been made using rotating disk electrodes of massive mineral samples. For comparative purposes, arsenopyrite, platinum and gold electrodes have also been used under the same conditions. The mixed potentials of the various minerals in solutions containing 4.2 mol/L sodium chloride, 0.1 mol/L hydrochloric acid and 0.054 mol/L iron(III) and/or 0.047 mol/L copper(II) ions at 25°C vary with time depending on the mineral reactivity. The difference between the mixed potentials and the solution potentials provide qualitative indications of mineral reactivity to dissolution with iron(III) or copper(II) as oxidants.

Cyclic voltammetry conducted at potentials negative to the mixed potentials at slow sweep rates after the mixed potential measurements has shown variable reactivity of the minerals for reduction of iron(III) and copper(II) ions. The data has been analysed in terms of electrochemical kinetics using a modified Butler-Volmer approach that takes into account mass transport of the oxidized and reduced species and anodic oxidation of the minerals. The electrochemical rate constant derived from a fit of the data to the rate

equation shows that all the minerals have greater reactivity for the reduction of copper(II) than iron(III) ions.

The rate constant varies by about an order of magnitude within the mineral group for both iron(III) and copper(II) reduction and the rate of reduction on platinum and gold electrodes are higher for both couples than for the mineral electrodes. The ratio of the rate of copper(II) reduction to iron(III) reduction is significantly greater for the minerals containing copper than for those without copper.

The observed influence of mass transport on the cathodic currents close to the mixed potentials for the reduction of copper(II) on platinum, pyrite and enargite has been quantitatively explained in terms of the effect of mass transport on the surface concentration of copper(I).

An attempt has been made to correlate the kinetic data with published data on the semi-conducting properties of the metal sulfides. With the exception of covellite (which is not considered a semiconductor), the formal potentials of the copper(II)/copper(I) and iron(III)/iron(II) couples fall within the bandgaps of the metal sulfides and there does not appear to be any correlation between the energy levels of the couples in solution relative to the conduction bands of the sulfides and the reactivity for electron transfer to the metal ion couples. The effect of illumination with light of wavelength 405nm on the cathodic currents has been demonstrated to be due to thermal and not photocurrent effects.

1. Introduction

The heap leaching of copper ores has become a well-established and important process option for oxide materials and, in recent years, attention has been focused on the

leaching of low grade sulfide ores. While this has been largely successful for secondary copper sulfides such as chalcocite and, to some extent, covellite, the slow leaching rates of the primary sulfides such as chalcopyrite and enargite remains an outstanding problem. Recent developments (Patino et al, 2014) in the application of chloride processes to the heap leaching of chalcopyrite have proved to be promising and this paper is the first of three which will deal with fundamental aspects of the dissolution of chalcopyrite and associated sulfide minerals in relatively concentrated chloride solutions. It is now generally accepted that the oxidative dissolution of sulfide minerals is electrochemical in nature and can be described by the mixed potential model in which anodic dissolution of the metal sulfide is coupled to cathodic reduction of an oxidant such as iron(III). The problem with chalcopyrite and enargite and, to a lesser extent other sulfide minerals such as covellite and pyrite is the formation of passive or partially passive metal sulfide layers that are formed under anodic oxidation particularly at the low temperatures typical of heap leaching. In the case of chalcopyrite, this can be avoided by operation at potentials below that at which so-called passivation occurs and enhanced rates of dissolution under controlled potential conditions in dilute chloride solutions have been demonstrated (Velásquez-Yévenes et al, 2010). Under these conditions, non-oxidative dissolution coupled to oxidation of sulfide/hydrogen sulfide by the oxidant has been suggested as an alternative mechanism of dissolution.

More recent unpublished but patented research and development (Patino et al, 2014) has demonstrated that direct oxidative dissolution of chalcopyrite can be successfully used in column and crib leaching of ores containing primarily chalcopyrite by increasing the chloride concentration in conjunction with other operating modifications. Fundamental studies have demonstrated that the mixed potential model applies under these conditions.

A fundamental description of the dissolution of chalcopyrite under these conditions requires knowledge of the mixed potentials, anodic dissolution characteristics of the mineral and the cathodic reduction of the oxidants which are both iron(III) and copper(II) in chloride solutions. A detailed study of the anodic processes will be the subject of a later paper while this paper will deal mainly with the cathodic processes. The presence of other sulfides such as covellite, enargite and pyrite in such ores requires that the study also include, in a more superficial way, the electrochemical behavior of these minerals under identical conditions. This first paper presents the results of a comparative study of the mixed potentials, voltammetric and potentiostatic measurements related to the reduction of iron(III) and copper(II) on these minerals in concentrated chloride solutions under identical conditions. Arsenopyrite has been included to provide an additional sulfide that does not contain copper while platinum and gold electrodes have also been added to the list as inert substrates for the cathodic reactions.

2. Experimental

2.1. Mineral electrodes

Mineral electrodes were prepared from natural samples of high purity that were cut into small cubes of side 5-10 mm. XRD analysis was used to confirm the purity of the samples and no impurity minerals could be detected by this technique in any of the samples. In the case of covellite, a synthetic sample was used as natural samples are invariably contaminated by chalcocite. The samples were fabricated as electrodes using silver epoxy as the contact of one face to a stainless steel stud that was encased in epoxy resin and machined to a cylindrical shape that was attached to the end of a rotating shaft whose speed was controlled. For photocurrent measurements, the electrodes were

inserted vertically in a small cell with the disk facing upward as described recently. (Nicol, 2016).

The DC resistivity (measured using the electrodes with a gold foil contact on the exposed face) and semiconductor type (obtained from the sign of the thermoelectric potential) for the various mineral samples are summarized in Table 1. The resistivity values should be viewed as approximate values for comparative purposes only.

Table 1. Electrical Properties of Mineral Samples

Mineral	Semiconducting Type	Resistivity Ohm cm
Arsenopyrite	p	34
Chalcopyrite	n	310
Covellite	metallic	1.5
Enargite	p	53
Pyrite	n	0.015

2.2. *Electrochemical measurements*

Electrochemical measurements were carried out using a standard three-electrode system with rotating working mineral electrodes. Potentials and currents were measured and controlled by a Solartron 1285 potentiostat operated with corrosion measurement software. The silver/silver chloride (3 mol/L KCl) reference electrode (0.207 V versus SHE) was separated by a Luggin capillary from the solution in the cell and the potentials were measured and controlled relative to this electrode at room temperature.

Electrolytes were prepared using 4.2 mol/L (150 g/L chloride) sodium chloride solutions containing 0.1 mol/L hydrochloric acid. This is referred to as the "base electrolyte". The solutions contained either 0.054 mol/L iron(III) or 0.047 mol/L copper(II) ions while measurements were also made with a solution containing 0.027 mol/L iron(III) and 0.024 mol/L copper(II) ions. These metal concentrations of 1.5 to 3 g/L were selected to approximate those obtained during heap leaching of ores containing copper sulphide minerals. Electrochemical measurements were carried out using the

5

following procedure. 50 cm^3 of electrolyte of the required composition was added to the cell and nitrogen bubbled through the solution for 15 min to deaerate the solution and allow the temperature to stabilize to 25°C. The electrodes were polished with 3000 grit water paper before each experiment. The appropriate electrode was immersed into the electrolyte and the mixed potential of the rotating electrode recorded for a period of 10 minutes. After measurement of the mixed potential, cyclic voltammetry was carried out at 1 mV/s from the rest potential in a negative direction and reversed when the current density approached -5 A/m^2. Potentiostatic experiments were conducted by immersing a freshly polished electrode in the solution, the potential set to the desired value and the resulting current recorded for 5 minutes at various rotation speeds. Unless otherwise stated, the electrodes were rotated at 200 rpm during the electrochemical measurements. The potentials were manually corrected for the voltage drop in each sample electrode using the resistance values as measured in the determination of the mineral resistivity. The voltage drop in the solution was negligible given the proximity of the Luggin capillary to the mineral surface and the high conductivity of the solutions. All potentials are shown relative to the standard hydrogen electrode (SHE).

The formal potentials of the iron(III)/iron(II) and copper(II)/copper(I) couples in 4 mol/L sodium chloride containing 0.1 mol/L hydrochloric acid were measured by constant current reduction of 0.05 mol/L solutions of iron(III) and copper(II) at a rotating gold disk electrode for various periods after which the solution potential was measured using the same reference electrode used in the other experiments. From the charge passed, the concentrations of iron(II) and copper(I) produced by the electrochemical reduction could be calculated and the formal potentials calculated using the Nernst equation. In this way, the formal potential of the iron(III)/iron(II) couple was measured as 0.695 V and that of the copper(II)/copper(I) as 0.565 V in the solution used.

3. Results and discussion

3.1. *Mixed potential measurements*

Figures 1 and 2 show the variation with time of the mixed potentials in solutions containing iron(III) or copper(II).
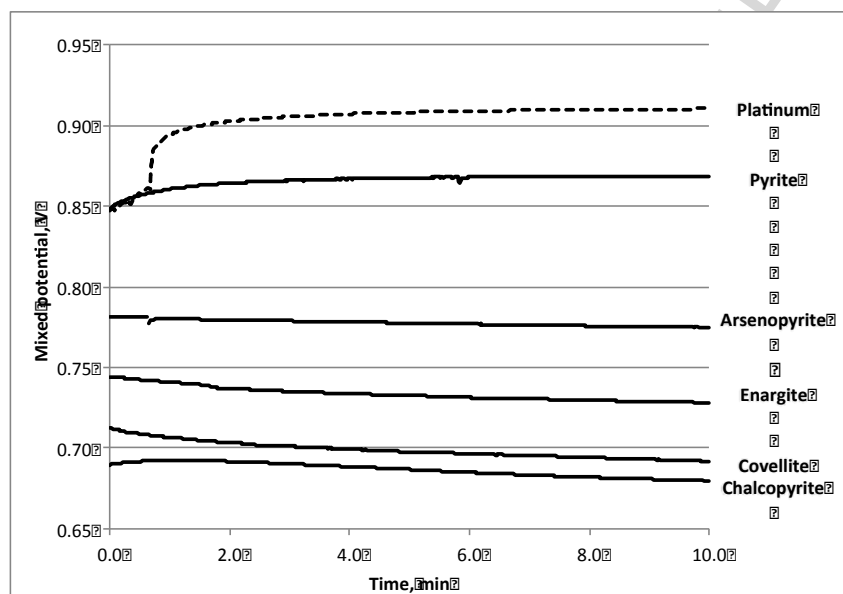

Figure 1. Mixed potentials of various mineral electrodes in the base electrolyte containing 3 g/L iron(III).
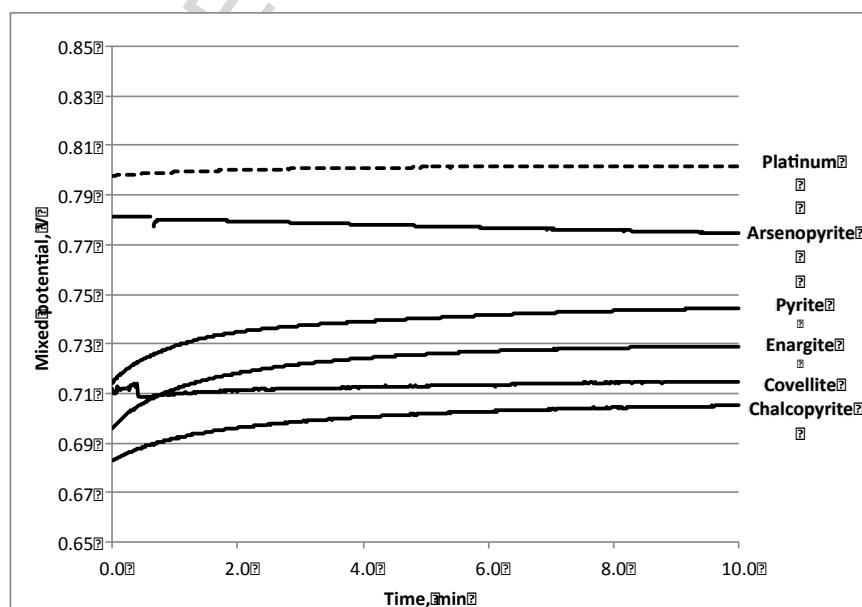

Figure 2. Mixed potentials of various mineral electrodes in the base electrolyte containing 3 g/L copper(II).

7

Figure 3 allows a comparison of all the potential data (including platinum) after 10 minutes.
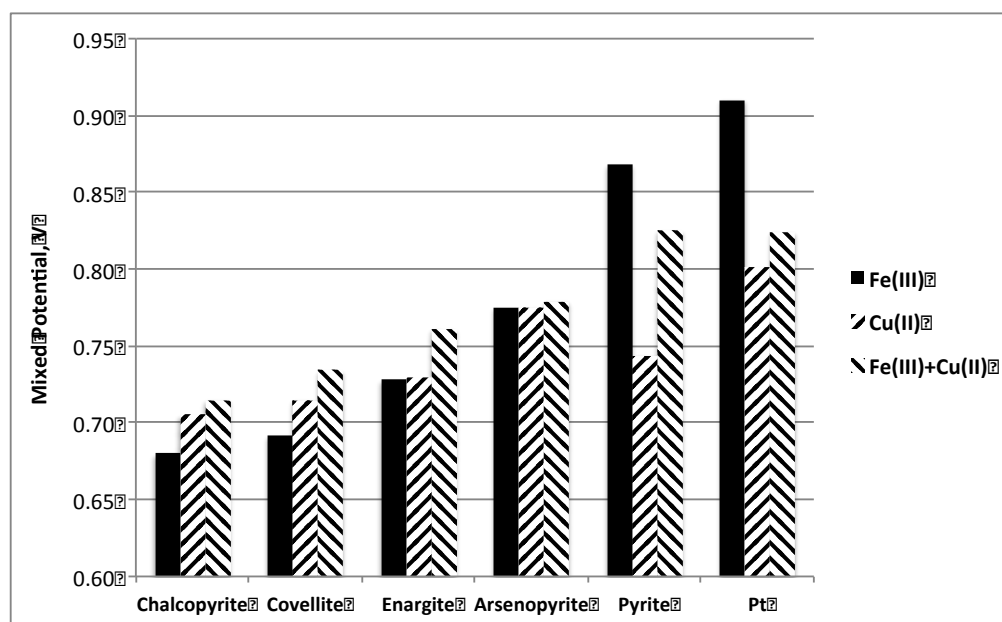

Figure 3. Mixed potentials after 10 minutes in base electrolyte with 3 g/L iron(III), 3 g/L copper(II) and 1.5 g/L of both metal ions.

In all cases, the mixed potentials are lower than the solution potentials as could be expected. This difference can be attributed to the formation of either iron(II) or copper(I) by oxidation of the mineral (Nicol and Lazaro, 2002). Because the potential of the iron(III)/iron(II) couple is higher than that for the copper(II)/copper(I) couple by some 0.13 V, the formation of a small amount of copper(I) from reaction of the mineral with copper(II) will have a greater impact on the mixed potential than formation of the same amount of iron(II). Except for pyrite, the potentials after 10 minutes are higher in the presence of copper(II) than iron(III) despite the fact iron(III) is a thermodynamically stronger oxidant than copper(II) by about 0.13 V. This is a qualitative indication that the rate of cathodic reduction of copper(II) is probably greater than that of iron(III) on all minerals. In the case of pyrite, the low anodic reactivity at potentials below about 0.7 V means that the mixed potential is at a value such that even a trace amount of copper(I) will lower the potential of the copper(II)/copper(I) couple. The mixed potentials in the

presence of both metal ions are higher in every case except pyrite. Under these conditions, the greater rate of reduction of copper(II) is coupled to the higher formal potential of the iron(III)/iron(II) couple by way of the rapid equilibrium

$$Cu(I) + Fe(III) = Cu(II) + Fe(II) \qquad K = 150 \ (4M \ NaCl \ at \ 25^{o}C)$$
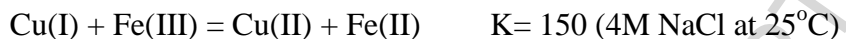
which maintains a low copper(I) concentration at the mineral surface and therefore a higher mixed potential.

3.2. *Linear sweep voltammetric measurements*

The results of the cathodic reduction of iron(III) and copper(II) on each of the minerals are shown in Figures 4 and 5 as linear sweep voltammograms obtained in a negative sweep direction from the mixed potentials. The data for gold is not shown as it was very similar to that for platinum.
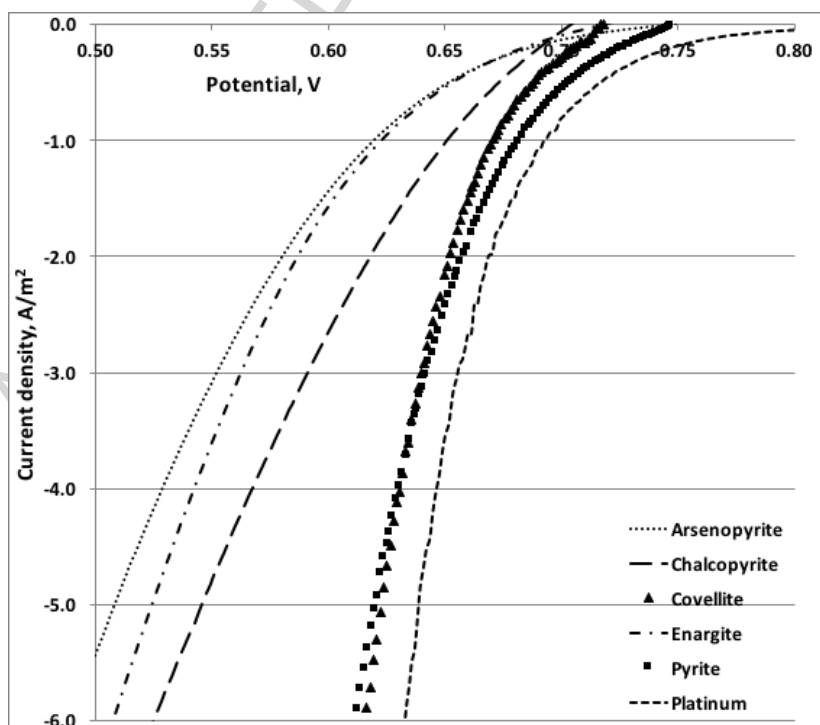

Figure 4. Linear sweep voltammograms for the minerals in base electrolyte containing 3 g/L iron(III).
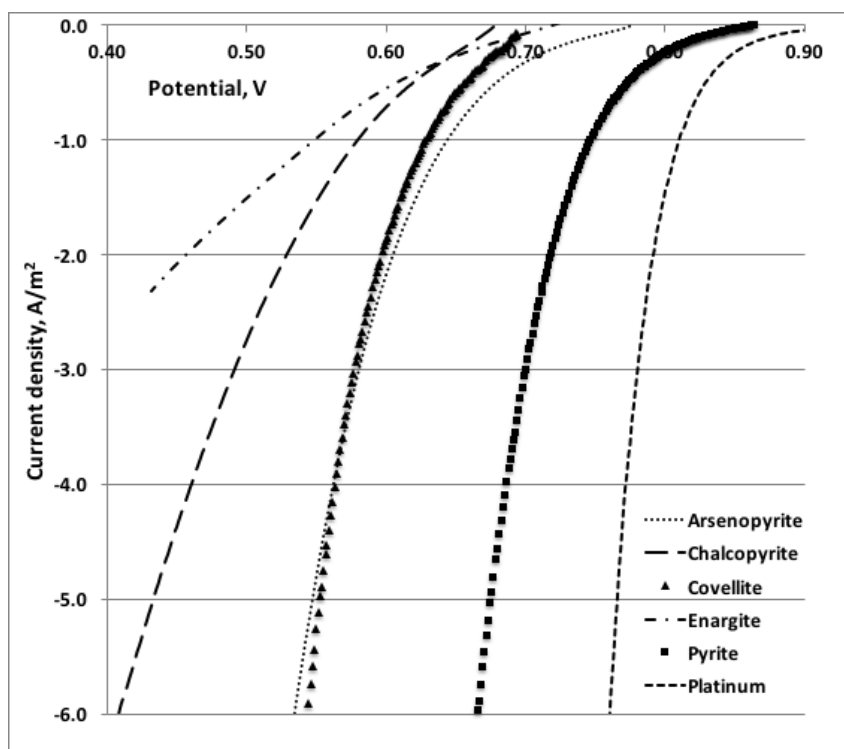
9

Figure 5. Linear sweep voltammograms for the minerals in base electrolyte containing 3 g/L copper(II).

For all minerals, currents in the absence of iron(III) or copper(II) at potentials in the region of interest i.e. a hundred millivolts negative to the mixed potentials were found to be small (less than 1% of the currents in the presence of iron(II) or copper(I) at the slow sweep rates used). Thus, contributions from simultaneous anodic oxidation (see Appendix) and possible cathodic reduction of the minerals can be neglected in comparison to the currents due to the reduction of iron(III) and copper(I). Hysteresis between the forward and reverse sweeps was small (less than 20 mV at -1 A/m^2) except in the case of iron(III) reduction on enargite in which case it was a maximum of 40 mV. Qualitatively, it can be seen that there are considerable differences in reactivity for reduction of both iron(III) and copper(II) amongst the different minerals with reduction of copper(II) ions being most rapid on covellite and pyrite while iron(III) reduction

10

occurs most rapidly on pyrite. The corresponding reactions on platinum and gold are, as expected, more reversible (in a kinetic sense) than on the mineral surfaces.

Quantitative comparisons can be made by fitting each of the curves in Figures 4 and 5 to an appropriate electrochemical rate expression. The derivation of the modified Butler-Volmer equation used for this purpose is given in the Appendix. Fits of the observed and calculated curves are shown in Figures 6 to 11 for each of the electrodes.

Figure 6. Observed (points) and calculated (line) i/E curves for the reduction of copper(II) and iron(III) on a chalcopyrite electrode. The dashed line is that calculated for the solution containing both metal ions.

Figure 7. Observed (points) and calculated (line) i/E curves for the reduction of copper(II) and iron(III) on an arsenopyrite electrode. The dashed line is that calculated for the solution containing both metal ions.

Figure 8. Observed (points) and calculated (line) i/E curves for the reduction of copper(II) and iron(III) on a pyrite electrode. The dashed line is that calculated for the solution containing both metal ions.

12
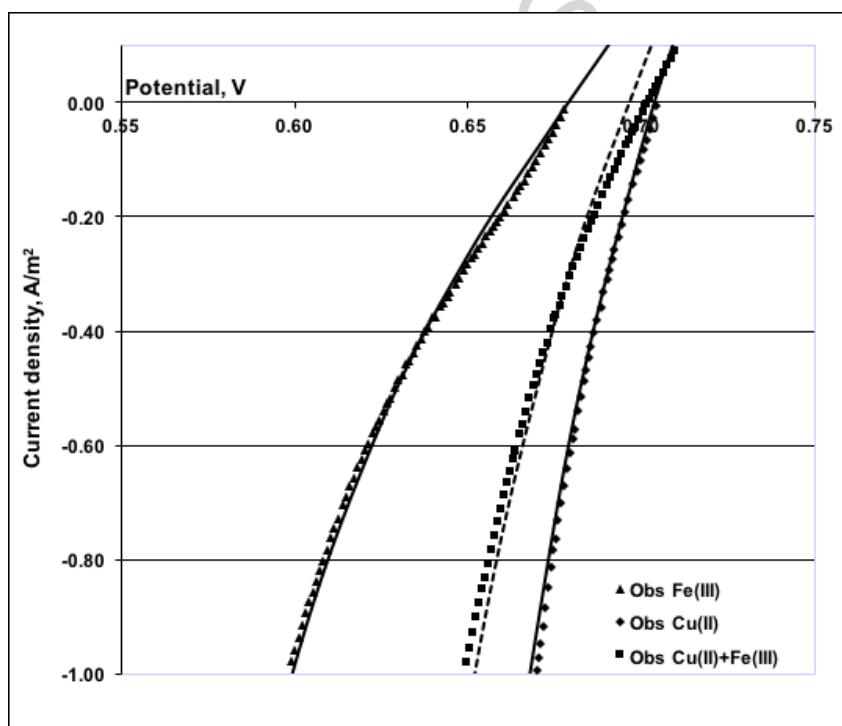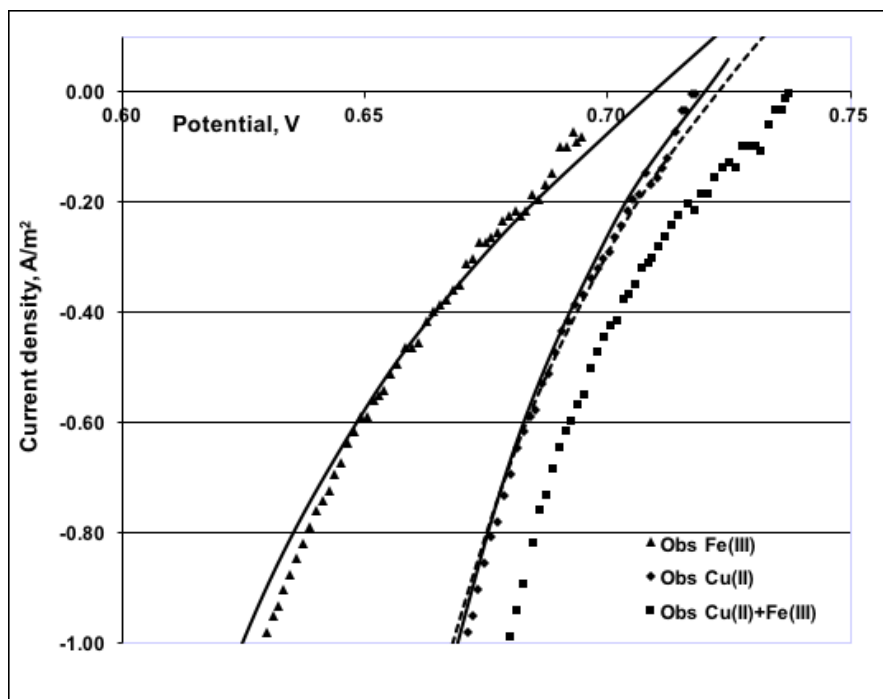
Figure 9. Observed (points) and calculated (line) i/E curves for the reduction of copper(II) and iron(III) on a covellite electrode. The dashed line is that calculated for the solution containing both metal ions.
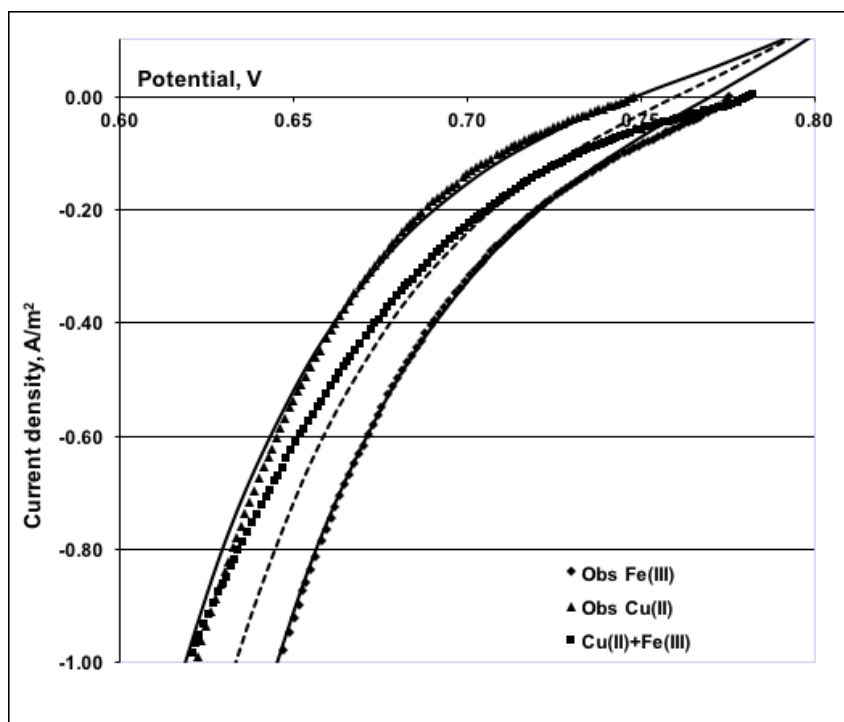

Figure 10. Observed (points) and calculated (line) i/E curves for the reduction of copper(II) and iron(III) on an enargite electrode. The dashed line is that calculated for the solution containing both metal ions.
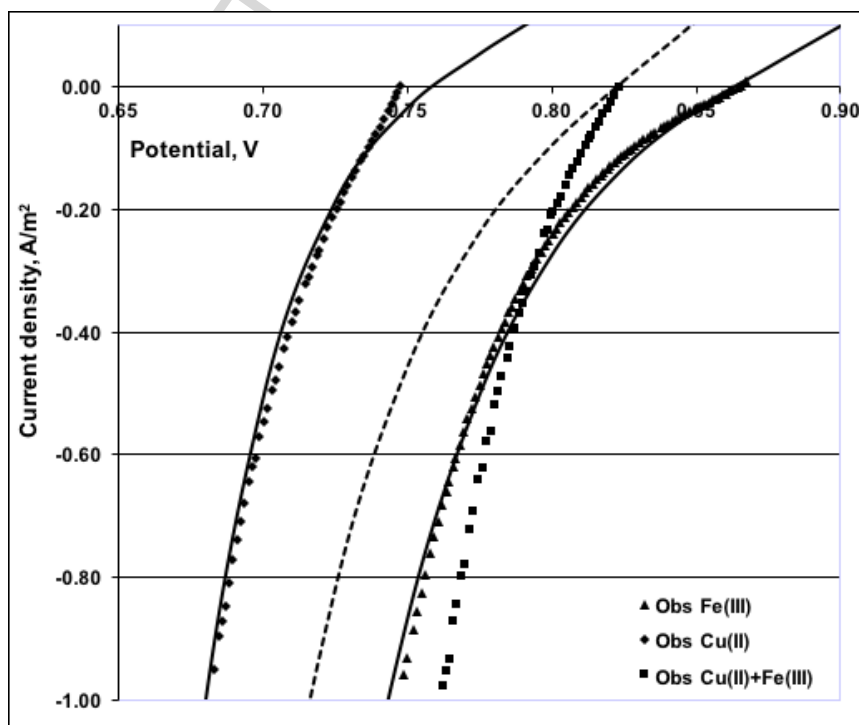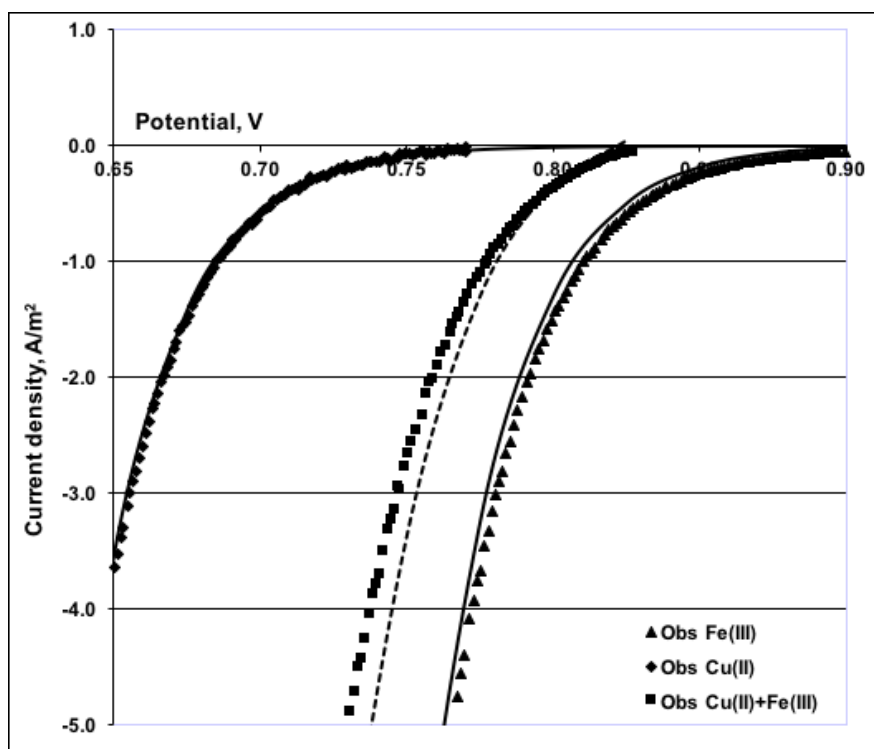
Figure 11. Observed (points) and calculated (line) i/E curves for the reduction of copper(II) and iron(III) on a platinum electrode. The dashed line is that calculated for the solution containing both metal ions.
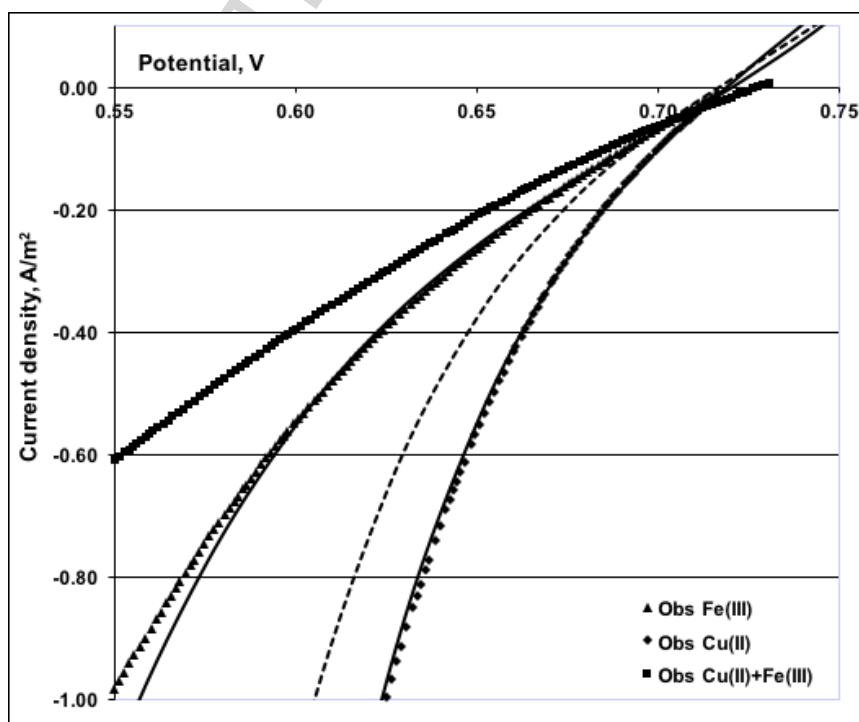
Comparison of the observed and calculated curves for the individual metal ions shows that, in general, the correspondence is very good considering that only two adjustable parameters (the electrochemical rate constants, k and k_a as defined in the Appendix) were used for each mineral with a different value for k in the case of iron(III) and copper(II). These rate constants for the cathodic reactions are summarized in Table 2.

Table 2. Electrochemical rate constants

Sulfide	Type	10^7 x k (m/s)		k_{Cu}/k_{Fe}
		Cu(II)/(I)	Fe(III)/(II)	
FeS_2	n	60	5.5	10.9
FeAsS	p	5.5	0.75	7.3
$CuFeS_2$	n	48	0.32	150
CuS	-	42	0.52	81
Cu_3AsS_4	p	7.8	0.18	43
Pt	-	>500	>500	-
Au	-	>500	65	>8

14

In all mineral cases, the rate of reduction of iron(III) is slower than that of copper(II) which contributes to a general observation that copper(II) is more effective for the oxidative leaching of these minerals in chloride solutions. It is clear that the rates of reduction of both iron(III) and copper(II) are greatest on a pyrite surface while copper(II) reduction is slowest on arsenopyrite and iron(III) reduction slowest on enargite. The ratio of the rates of reduction of copper(II) to iron(III) is significantly greater for those minerals containing copper. It remains to be established by similar studies on additional mineral sulfides whether this is a more general observation. The similar rates of reduction of iron(III) and, particularly, copper(II) on chalcopyrite and covellite surfaces is interesting in that recent studies have suggested that the chalcopyrite surface is possibly converted to a covellite-like state in acid solutions, particularly in the presence of copper ions. (Nicol et al, 2010; Muszer et al, 2013; Zeng et al, 2013). The faster reduction of copper(II) than iron(III) is also apparent in the data for platinum and gold electrodes. In the case of platinum and gold (for copper(II) reduction), the curves are approaching those for a kinetically reversible system ($k > k_L$) and the rate constants cannot be determined accurately using voltammetric data. Thus only lower limits can be used.

The data in Table 2 are useful in another respect. The oft-quoted galvanic effect that results in increased dissolution of minerals in the presence of, say, pyrite because of assumed greater rates of the cathodic reactions on a pyrite surface in contact with the dissolving mineral can be assessed by comparing the values for pyrite with the other sulfides in Table 2. It could be expected that pyrite would not show catalysis of chalcopyrite or covellite dissolution with copper(II) as the oxidant in chloride solutions because the rates of the cathodic reactions are similar but could possibly do so in all other cases with both copper(II) and iron(III) as the oxidants. However, the process is

more complex in that it requires that the pyrite be in electrical contact with the dissolving mineral for a significant fraction of the time in a stirred slurry and that the surface area of the pyrite be large enough to have a measurable effect on the rate of dissolution.

3.3.   Mass transfer effects.

It is not generally appreciated that the degree of agitation can, in some cases, have an effect on the cathodic (or anodic) currents at potentials which are close to the equilibrium (or mixed) potential i.e. at current densities that are very much lower than the limiting current density for the reduction of an oxidant such as copper(II) or iron(III). This will occur in cases for which the rates of reduction are relatively high such as observed with pyrite. Initial measurements with pyrite showed that the current density appeared to vary with agitation even at potentials very close to the mixed potential. In fact, the mixed potential itself increases with increased rotation speed of the electrode. A similar effect was observed in a sulfate system but not explained in a recent publication (Nicol et al, 2013). Potentiostatic measurements were therefore made on pyrite, enargite and platinum electrodes in a solution of 3 g/L copper(II) in the base electrolyte. The potential was controlled at 0.60 and 0.65 V in the case of pyrite, 0.60 V for enargite and 0.70 V for platinum at various rotation speeds and the steady current densities measured. The results are plotted in Figure 12 as the reciprocal of the current density versus the reciprocal of the square root of the rotation speed. The linear relationship is predicted from equations (8) and (9) in the Appendix under conditions such that the current density (i) is very much less than the limiting current density (i_L) for the reduction of copper(II).
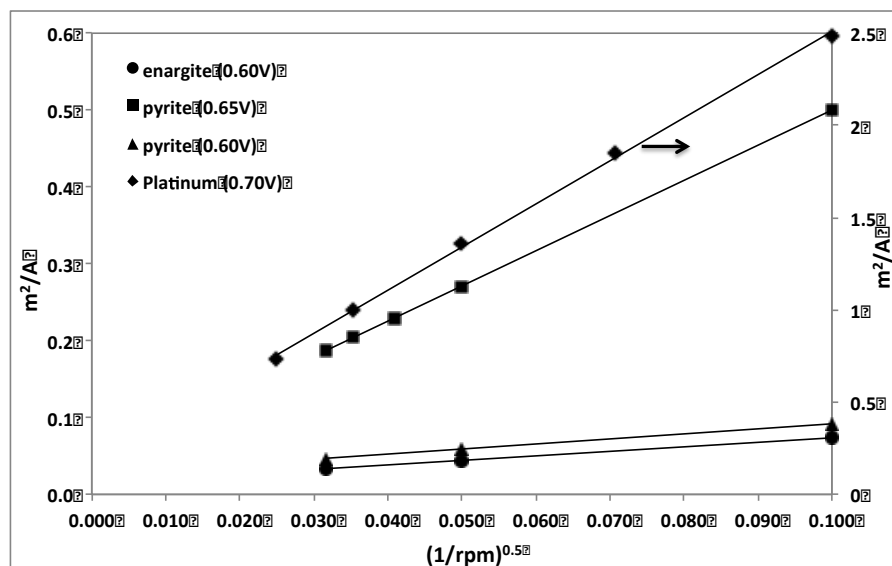
Figure 12. Effect of mass transport on the cathodic currents for reduction of copper(II) ions on pyrite, enargite and platinum.

The origin of this effect is that the reverse reaction of anodic oxidation of copper(I) occurs simultaneously with the cathodic reduction of copper(II) at these potentials and the rates of each are equal at the equilibrium potential. In this case, copper(I) is not present in the bulk of the solution but is produced by reduction of copper(II) at the surface of the electrode. As the rotation speed increases, this copper(I) is removed more rapidly from the surface of the electrode and the anodic current for oxidation of copper(I) is thereby diminished with a resulting increased net cathodic current. This effect is taken into account in the calculated curves shown in Figures 6 to 11.

Observation of this effect depends on the rate of electron transfer to the copper(II)/copper(I) couple. With the exception of pyrite, no noticeable effect of rotation speed was observed with any of the minerals for reduction of iron(III) which can be predicted given the relatively low degree of reversibility (Table 2) for this reaction.

3.4.   Simultaneous reduction of both copper(II) and iron(III).

It could be expected that reduction of a mixture of both iron(III) and copper(II) in solution would yield cathodic currents which would be the sum of the currents for reduction of each metal ion separately.

Included in Figures 6 to 11 are the observed curves for the reduction of a solution containing 3 g/L each of iron(III) and copper(II) together with those calculated assuming that the overall current is simply the sum of the contributions of each metal ion. In these calculations, the kinetic parameters used are the same as derived for reduction of the single metal ions and the processes are reasonably considered first-order in the concentration of the metal ions. A comparison of the observed and calculated curves shows that this simple interpretation is not generally correct with the magnitude of the observed currents being higher than calculated in the case of pyrite and covellite, approximately equal for arsenopyrite, chalcopyrite and platinum and significantly lower for enargite.

A possible explanation for the greater currents observed in the case of pyrite and covellite is that oxidation of copper(I) ions (produced by cathodic reduction of copper(II)) is reduced in the presence of iron(III) ions as a result of rapid oxidation (Orth and Liddell, 1990; Miki and Nicol, 2008) by the reaction

$$Fe(III) + Cu(I) = Fe(II) + Cu(II)$$
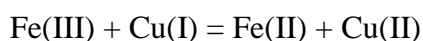
Thus, the current due to anodic oxidation of copper(I) is reduced with a resulting increased net cathodic current. The reason for the reduced currents in the case of enargite are not known at this stage.

3.5. *Relationship to semiconducting properties.*

Recent publications (Crundwell, 2013; Crundwell, 2014) have re-visited previous claims (Crundwell, 1988; Misra and Osseo-asare, 1988) that the semiconducting properties of sulfide minerals such as those employed in this study are both relevant and

important in determining the mechanisms and reactivities of these minerals towards leaching. The results of this study are therefore interesting from this perspective. Figure 13 summarizes the energy levels of the various sulfide minerals (converted from the Absolute Vacuum Scale) using published data (Xu and Schoonen, 2000) for pH 2. In this diagram, the lowest energy level in the conduction band is shown at the top of each vertical column and highest energy level in the valence band at the bottom of each column. No corrections have been made for the effect of pH which are relatively minor and because of the non-availability of data for correction for all except pyrite (correction 28 mV) and chalcopyrite (correction 47 mV). Also shown are the formal potentials for the copper(II), iron(III) and oxygen couples in solution on the same scale.

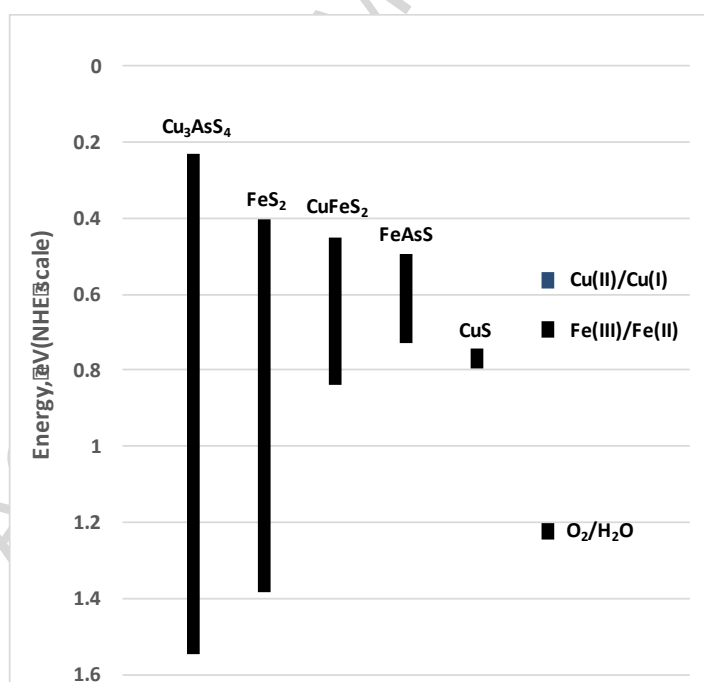Figure 13. Mineral semiconductor energy levels (converted from absolute vacuum scale at pH 2) and formal potentials in solution. The black area for each mineral is the bandgap.

In terms of accepted semiconductor electrochemistry theory, electron transfer between redox couples in solution and the conduction band of the semiconductor requires that the formal potential lie at energy levels within or close to the conduction band energy

levels. It is clear from Figure 13 that this requirement is not satisfied for any of the sulfides except covellite that is, in any case, believed to have a bandgap of zero. On this basis, low rates of electron transfer to copper(II)/copper(I) and iron(III)/iron(II) would be predicted whereas the results in Table 2 show relatively high rates of reduction in comparison with the metal electrodes.

Thus, the most reactive mineral for reduction of both iron(III) and copper(II) is pyrite despite the fact that the unfavourable difference between the relevant energy levels is about 0.2 eV for copper(II) and 0.3 eV for iron(III). In this regard, it should be pointed out that the position of the copper(II)/copper(I) couple in chloride solutions shown in previously published work (Crundwell, 1988, 2014) is in error in that the potential of the couple in a non-complexing medium (0.155 V) was used instead of the significantly higher potential in chloride media. This was incorrectly used to explain the greater reactivity for copper(II) as an oxidant for chalcopyrite in chloride media.

By comparing the data in Table 2 with that in Figure 13, it is not difficult to come to a conclusion that there does not appear to be any correlation between the semiconducting properties (n- or p-type, resistivity or energy levels) and reactivity for reduction of copper(II) and iron(III). This conclusion supports that of several previous studies that showed no correlation between the semiconducting properties of some of these minerals and both electrochemical reactivity (anodic and cathodic examples) and leach kinetics. (Biegler, 1976; Klein and Shuey, 1978; Biegler and Swift, 1979; Springer, 1970; Dutrizac, 1982; Kelsall et al, 1996; Lehner et al, 2007).

The probable explanation for the lack of influence of semiconducting properties on reactivity is related to the impurity metals present even in single phase natural sulfide minerals. The total metal impurity content can often exceed several parts per million-a level that is orders of magnitude greater than semiconductor grade synthetic materials.

This can result in many impurity energy levels within the band gap of a natural material that, in turn, can produce a complex and non-predictable band structure. Pseudo-metallic behaviour can be a consequence of this particularly for those materials that have small band gaps (Lehner et al, 2007; Gerischer, 1972). Thus, the structures shown in Figure 13 are unlikely to be a true reflection for even high quality natural samples.

In a recent publication (Crundwell et al, 2015) it has been suggested, on the basis of photocurrents and the variation of capacitance with potential, that in the case of chalcopyrite in dilute sulfuric acid, semiconducting effects are responsible for the anodic behaviour and "passivation" of the mineral. In order to evaluate whether this could apply to the cathodic reactions in chloride solutions, several experiments were conducted using a low wavelength laser diode as the source of illumination. Figure 14 shows the positive-going portion (from 0.57 V) of the cyclic voltammogram of chalcopyrite in a solution of 4 mol/L sodium chloride containing 0.02 mol/L each of iron(II), iron(III) and hydrochloric acid. The sweep, at 0.1 mV/s, was initiated in a negative direction from the rest potential and the electrode was illuminated by a violet (405 nm) laser diode that was switched on every 200 s for a period of 30 s. Simultaneously, the temperature of the mineral surface was monitored by a micro-thermistor probe resting on the exposed face of the electrode. Details of this procedure have recently been published. (Nicol, 2016).
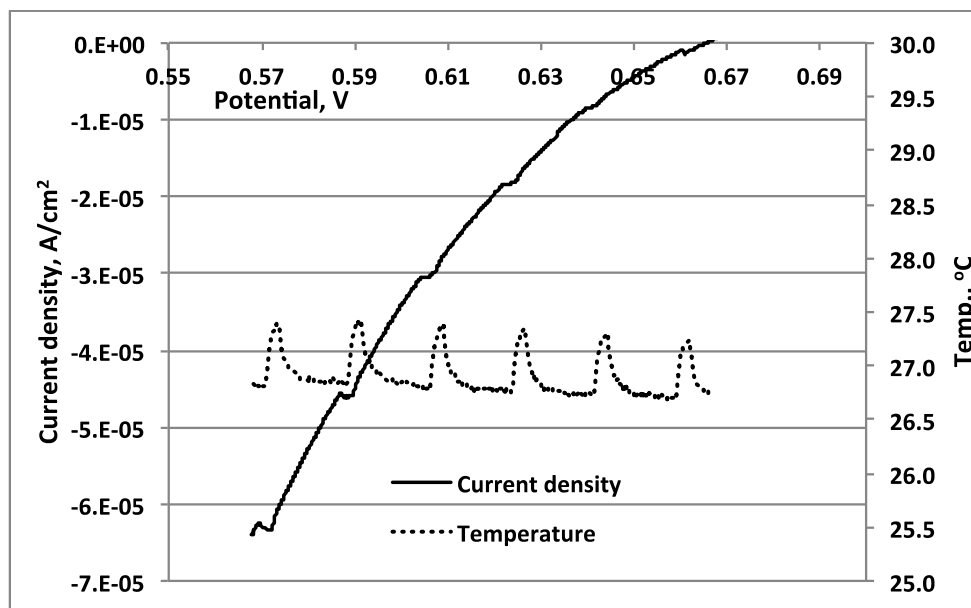
Figure 14. Linear sweep voltammogram (in positive direction) for the reduction of iron(III) on chalcopyrite in base electrolyte containing 0.02 mol/L each of iron(III) and iron(II). The electrode was periodically illuminated by a violet laser diode and the temperature of the surface simultaneously monitored.

The small negative deviations during illumination by the laser are accompanied by an increase in temperature of the mineral surface of at least $0.5^{\circ}C$. This increase in temperature can account for the increased (in absolute terms) currents that cannot therefore be ascribed to photocurrents.

Although photocurrents would not be expected to be observed for a cathodic reaction involving an n-type semiconductor such as chalcopyrite, a photo-response could be obtained with p-type semiconductors such as enargite with a bandgap of 1.28 eV (equivalent wavelength 969 nm) and arsenopyrite with a bandgap of 0.20 eV (equivalent wavelength 6200 nm). Figure 15 shows the result of a similar experiment with arsenopyrite to that shown in Figure 14 for chalcopyrite.
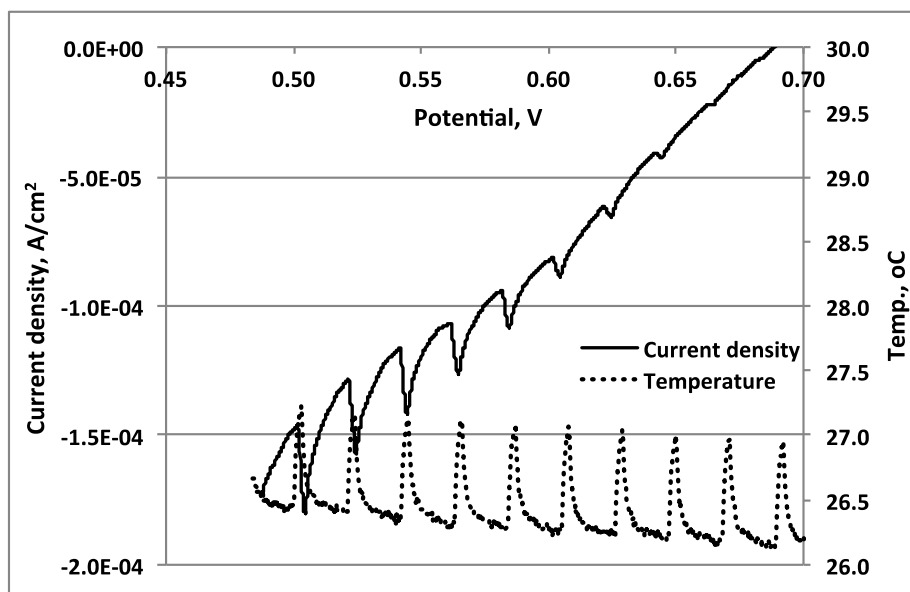
Figure 15. Linear sweep voltammogram (in negative direction) for the reduction of iron(III) on arsenopyrite in base electrolyte containing 0.02 mol/L each of iron(III) and iron(II). The electrode was periodically illuminated by a violet laser diode and the temperature of the surface simultaneously monitored.

In this case there do appear to be significant increases in the cathodic currents at potentials below about 0.6 V that increase with increasing absolute current density. However, assignment of these changes to photocurrents is not necessarily correct given the significant (almost 1°C) measured temperature change and also to the fact that the current densities in this region are close to the limiting current which has been estimated as being between 1.5×10^{-4} and 2×10^{-4} A/cm^2 (Cussler, 2009). Thermal convection at the upward-facing disk electrode will result in increased limiting currents under illumination. In order to verify this, a gold disk electrode was used and the same experiment repeated with the result shown in Figure 16.
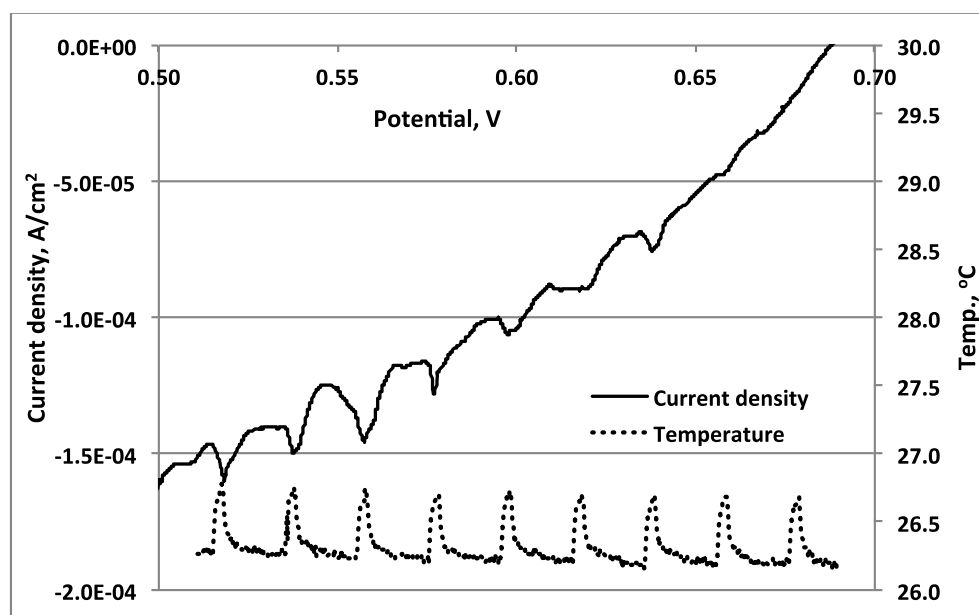
Figure 16. Linear sweep voltammogram (in a positive direction) for the reduction of iron(III) on gold in base electrolyte containing 0.02 mol/L each of iron(III) and iron(II). The electrode was periodically illuminated by a violet laser diode and the temperature of the surface simultaneously monitored.

Although the shapes of the current and temperature profiles during illumination of gold and arsenopyrite electrodes are not identical as could be expected given the different heat capacity and thermal conductivities of these materials, the increased currents at potentials approaching the limiting current region can only be ascribed to mass transfer effects and not photocurrents at the metallic electrode. The absence of such effects with chalcopyrite (Figure 14) are due to the lower current densities that are well below the limiting current. Similar results were obtained with enargite.

These results support the other conclusions made in this paper that the semiconducting properties of the sulfide minerals tested are not important in determining their electrochemical response during cathodic reactions in acidic chloride solutions at ambient temperatures.

4. Conclusions

A comparative study of the electrochemical reduction of iron(III) and copper(II) ions on selected sulfide mineral, platinum and gold rotating disk electrodes in concentrated chloride solutions has been carried out.

The mixed potentials of the various minerals in solutions containing 4.2 mol/L sodium chloride, 0.1 mol/L hydrochloric acid and 3 g/L iron(II) and/or 3 g/L copper(II) ions at $25^{o}C$ vary with time depending on the mineral reactivity. The difference between the mixed potentials and the solution potentials provided qualitative indications of mineral reactivity to dissolution with iron(III) or copper(II) as oxidants.

Cyclic voltammetry conducted at potentials negative to the mixed potentials at slow sweep rates after the mixed potential measurements has shown variable reactivity of the minerals for reduction of iron(III) and copper(II) ions. The data has been analysed in terms of conventional electrochemical kinetics using a modified Butler-Volmer approach that takes into account mass transport of the oxidized and reduced species. The electrochemical rate constant derived from a fit of the data to the rate equation shows that all the minerals have greater reactivity for the reduction of copper(II) than iron(III) ions. The rate constants vary by over an order of magnitude within the mineral group for both iron(III) and copper(II) reduction and the rate of reduction on platinum and gold electrodes are higher for both couples than for the mineral electrodes. The ratio of the rate of copper(II) reduction to iron(III) reduction is significantly greater for the minerals containing copper than for those without copper.

Rates of reduction using an equimolar solution of both metal ions are similar to those predicted assuming that the overall current is the sum of the contributions from each metal ion for platinum, arsenopyrite and chalcopyrite. In the case of pyrite and covellite, the predicted rates are significantly lower than observed and this has been described in

25

terms of the oxidation of copper(I) (formed by cathodic reduction of copper(II)) by iron(III) by the rapid reaction

Fe(III) + Cu(I) = Cu(II) + Fe(II)
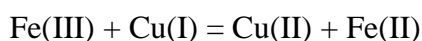
In the case of enargite, the predicted rate is higher than that observed but no explanation is obvious at this time.

The observed influence of mass transport on the cathodic currents close to the mixed potentials for the reduction of copper(II) on platinum, pyrite and enargite has been explained in terms of the effect of mass transport on the surface concentration of copper(I). Reduced surface concentrations at increased rotation speeds results in lower anodic currents for the oxidation of copper(I) and therefore increased net cathodic currents. Potentiostatic measurements at different rotation speeds provided data that is consistent with that predicted by the electrochemical rate equations.

An attempt has been made to correlate the kinetic data with published data on the semi-conducting properties of the metal sulfides. With the exception of covellite (which is generally not considered a semiconductor), the formal potentials of the copper(II)/copper(I) and iron(III)/iron(II) couples fall within the bandgaps of all the metal sulfides and there does not appear to be any correlation between the energy levels of the couples in solution relative to the conduction bands of the sulfides and the reactivity for electron transfer to the metal ion couples. In addition, increases in cathodic currents during illumination have been ascribed to and verified as thermal and not photocurrent effects.

5. Appendix

The following treatment follows that presented in an excellent text on electrochemical kinetics (Oldham and Myland, 1994).

The cathodic reactions can be written in the general form

$$Ox + e = Red \tag{1}$$

and the kinetics are best described by the Butler-Volmer equation which is conveniently written in the form

$$i = -Fk_f[\ [Ox]_s \exp\{(-\alpha F(E - E_f)/RT\} - [Red]_s \exp\{(1-\alpha)F(E - E_f)/RT\}] \tag{2}$$

in which,

i is the current density (A/cm^2),

F is the Faraday constant (96480 A.s/mol),

k is a potential independent electrochemical rate constant (cm/s),

$[Ox]_s$ is the concentration of the oxidised species at the electrode surface (mol/cm^3),

α is the so-called transfer coefficient (assumed to be 0.5 in all cases),

E is the potential with respect to any reference electrode, V

E_f is the formal (or conditional) potential for the particular solution under study defined as the equilibrium potential at $[Ox] = [Red]$ using the same reference electrode.

Note   (1) The net negative current by convention for cathodic processes.

(2) At $E = E_f$,

$$i = -Fk\ (\ [Ox]_s - [Red]_s\ ) = 0\ \ for\ [Ox]_s = [Red]_s \tag{3}$$

$$i.e.\ -Fk\ [Ox]_s = Fk\ [Red]_s = i_{o,f} \tag{4}$$

in which $i_{o,f}$ is the exchange current density (A/cm^2) at the formal potential.

The surface concentrations of the reacting species will not be equal to the bulk concentrations because of generation or consumption by the electrochemical reactions. Thus, using Fick's First Law, one can write

27

$$[Ox]_s = [Ox]_o + i/Fk_L^O \tag{5}$$

$$[Red]_s = [Red]_o - i/Fk_L^R \tag{6}$$

in which,

$[Ox]_o$ is the bulk concentration of Ox (mol/cm^3) and

k_L^O is the mass transfer coefficient (cm/s) for transport of Ox to the surface of the electrode.

For a rotating disk electrode, the mass transfer coefficient for Ox (similar equations for mass transport of Red) is given by the Levich equation

$$k_L^O = 0.620 \, v^{1/6} \, D_{Ox}^{2/3} \, w^{1/2} \tag{7}$$

in which,

v is the kinematic viscosity of the solution (cm^2/s),

D_{Ox} is the diffusion coefficient of Ox (cm^2/s)

w is the rotation speed of the electrode (radian/s)

Equations (5) and (7) (and the equivalent equations involving Red) can be substituted into (2) to give (after some mathematical manipulation),

$$i = -\frac{F\exp(-\alpha f(E))\{[Ox]_o - [Red]_o \exp\{f(E)\}}{\frac{1}{k} + \frac{\exp\{(1-\alpha)F(E)\}}{k_L^R} + \frac{\exp\{-\alpha f(E)\}}{k_L^O}} \tag{8}$$

in which $f(E) = F(E-E_f)/RT$

In the present case the solution only contained the Ox species, in which case, the above can be written in the following form by setting $[Red]_o = 0$,

$$1/i = 1/i_c + 1/i_{ap} + 1/i_L \tag{9}$$

in which

$$i_c = -Fk \, [Ox]_o / \exp\{\alpha f(E)\} \tag{10}$$

$$i_{ap} = -F \, k_L^R \, [Ox]_o / \exp\{f(E)\} \tag{11}$$

$$i_L = -F \, k_L^O \, [Ox]_o \tag{12}$$

28

i_C is the equation for the reduction of Ox in the absence of mass transport restrictions

i_{ap} is related to the contribution of the back reaction (oxidation of Red) to the overall current density

i_L is the limiting current density for the reduction of Ox.

The relative contributions of each term to the overall current density will depend on the magnitude of each term with the smallest being the most important.

At potentials close to the mixed potential, the anodic current due to oxidation of the mineral has also to be taken into account. This can be included by making the assumption that the anodic current density is given by

$i_a = Fk_a \exp\{((1-\alpha)F(E - E_a)/RT\}$

in which

k_a is a potential independent electrochemical rate constant (cm/s) that incorporates the number of electrons (n) in the rate-determining step.

E_a is the formal potential under the conditions of the experiments for the following assumed reactions (the stoichiometry and potentials do not affect the calculations that involve selection of a suitable k_a value to fit the observed curves close to the mixed potential)

Reaction	Ea, V
$CuFeS_2 = Cu(II) + Fe(II) + 2S + 4e$	0.420
$FeS_2 = Fe(II) + 2S + 2e$	0.390
$CuS = Cu(II) + S + 2e$	0.618
$FeAsS + 3H_2O = Fe(II) + H_2AsO_3^- + S + 4H^+ + 5e$	0.283
$Cu_3AsS_4 + 3 H_2O = 3Cu(II) + H_2AsO_3^- + 4S + 4H^+ + 9e$	0.749

The other symbols have the same meaning as above.

The diffusion coefficients in the base electrolyte were calculated from the Levich equation using the measured limiting current densities on a rotating platinum disk electrode in solutions containing the same concentrations of copper(II) and iron(III).

6. References

Biegler T. 1976. Oxygen reduction on sulfide minerals Part II Relation between activity and semiconducting properties of pyrite electrodes. J. Electroanal. Chem. 70: 265-275

Biegler T. and Swift D.A. 1979. Anodic behaviour of pyrite in acid solutions. Electrochim. Acta. 24: 415-420

Crundwell F.K. 1988. The influence of the electronic structure of solids on the anodic dissolution and leaching of semiconducting sulphide minerals. Hydrometallurgy. 21: 155-190

Crundwell F.K. 2014. The semiconductor mechanism of dissolution and the pseudo-passivation of chalcopyrite. *Hydrometallurgy 2014*, The Minerals, Metals and Materials Society, Warrendale, Pennsylvania, 1: 351-362

Crundwell F.K. 2013. The dissolution and leaching of minerals: Mechanisms, myths and misunderstandings. Hydrometallurgy. 139: 132-148

Crundwell, F.K.,van Aswegen, A., Bryson, L.J., Biley,C., Craig, D., Marsicano, V.D. and Keartland, J.M. 2015. The effect of visible light on the dissolution of natural chalcopyrite ($CuFeS_2$) in sulphuric acid solutions. Hydrometallurgy 158: 119-131.

Cussler E.L. 2009. Diffusion (3rd ed). Cambridge University Press. p254.

Dutrizac J.E. 1982. Ferric ion leaching of chalcopyrites from different localities. Metall. Trans B. 13B: 303-309

Gerischer, H. 1972. Personal communication.

Kelsall G.H., Yin Q., Vaughan D.J. and England K.E.R. 1996. Electrochemical oxidation of pyrite (FeS$_2$) in acidic aqueous electrolytes i. In Electrochemistry in Mineral and Metal Processing IV (eds. F.M.Doyle, P.E.Richardson and R.Woods). The Electrochemical Society. 131-142

Klein J.D. and Shuey R.T. 1978, Non-linear impedance of mineral electrolyte interfaces. Part 1. Pyrite. Geophysics 43: 1222-1234

Lehner S., Savage K., Ciobanu M. and Cliffel D.E. 2007. The effect of As, Co and Ni impurities on pyrite oxidation kinetics: An electrochemical study of synthetic pyrite. Geochim. Cosmochim. Acta 71: 2419-2509

Miki H. and Nicol M.J. 2008. Synergism in the oxidation of covellite and pyrite by iron(III) and copper(II) ions in chloride solutions. *Hydrometallurgy 2008*, The Minerals, Metals and Materials Society, Warrendale, Pennsylvania, 646-652

Misra K.K. and Osseoasare, K. 1988. Aspects of the interfacial electrochemistry of semiconductor pyrite (FeS$_2$). J. Electrochem. Soc. 135: 2502-2509

Muszer A., Wodka J., Chmielewski T. and Matuska S. 2013. Covellinisation of copper sulfide minerals under pressure leaching conditions. Hydrometallurgy. 137:1-7

Nicol M.J. and Lazaro I. 2002. The role of Eh measurements in the interpretation of the kinetics and mechanisms of the oxidation and leaching of sulfide minerals. Hydrometallurgy. 63: pp 15-22

Nicol M.J., Miki H. and Velásquez-Yévenes L. 2010. The dissolution of chalcopyrite in chloride solutions. Part 3. Mechanisms. Hydrometallurgy. 103: 86-95

Nicol M., Miki H., Zhang S. and Basson P. 2013. The effects of sulfate ions and temperature on the leaching of pyrite. 1. Electrochemistry. Hydrometallurgy 133: 188-196

Nicol M.J. 2016. Photocurrents at chalcopyrite and pyrite electrodes under leaching conditions. Hydrometallurgy , 163: 104-107

Oldham K.B. and Myland J.C. 1994. "Fundamentals of Electrochemical Science" Academic Press, 1250 Sixth Ave. San Diego, California.

Orth R.J. and Liddell K.C. 1990. Rate law and mechanism for the oxidation of copper(I) by iron(III) in hydrochloric acid solutions. Ind. Eng. Chem. Res. 29:1178-1184

Patino M.E., Nicol, M.J., Rautenbach, G.F. 2014. Heap Leaching Method. PCT Int. Appl., 9pp. CODEN: PIXXD2 WO 2014030048 A1 PCT IB2013/001810

Springer G. 1970.   Observations on the electrochemical reactivity of semiconducting minerals. Trans. Inst. Mining Metall. Sect. C 79: c11-c15

Velásquez-Yévenes L., Nicol M.J. and Miki H. 2010. The dissolution of chalcopyrite in chloride solutions. Part 1. Effect of solution potential. Hydrometallurgy 103: 108-113

Xu Y. and Schoonen A.A.   2000. The absolute energy positions of conduction and valence bands of selected semiconducting minerals. American Mineralogist 85: 543-556.

Zeng W. Qiu G. and Chen M. 2013. Investigation of CuS intermediate species during electrochemical dissolution and bioleaching of chalcopyrite concentrate. Hydrometallurgy. 134: 158-165

Highlights

Comparative study of the electrochemical reduction of iron(III) and copper(II) ions on chalcopyrite, covellite, enargite, pyrite and arsenopyrite in chloride solutions.

The voltammetric data analysed in terms of electrochemical kinetics using a modified Butler-Volmer approach that takes into account mass transport of the oxidized and reduced species.

The electrochemical rate constant shows that all the minerals have greater reactivity for the reduction of copper(II) than iron(III) ions.

The rate constant varies by about an order of magnitude within the mineral group for both iron(III) and copper(II) reduction

The ratio of the rate of copper(II) reduction to iron(III) reduction is significantly greater for the minerals containing copper than for those without copper.

The observed influence of mass transport on the cathodic currents close to the mixed potentials for the reduction of copper(II) on platinum, pyrite and enargite has been quantitatively explained in terms of the effect of mass transport on the surface concentration of copper(I).

There do not appear to be any semiconducting effects on the reduction of iron(III) or copper(II) on these minerals.